

Higgs hunting with B decays*

Ulrich Nierste^a

^a Institut für Theoretische Teilchenphysik (TTP)
Karlsruhe Institute of Technology (Universität Karlsruhe),
76131 Karlsruhe, Germany

B physics is sensitive to the effects of Higgs bosons in the Minimal Supersymmetric Standard Model, if the parameter $\tan\beta$ is large. I briefly summarise the role of $B \rightarrow \mu^+\mu^-$ and $B^+ \rightarrow \tau^+\nu_\tau$ in the hunt for new Higgs effects and present new results on the decay $B \rightarrow D\tau\nu_\tau$: Using the analyticity properties of form factors one can predict the ratio $R \equiv \mathcal{B}(B \rightarrow D\tau\nu_\tau)/\mathcal{B}(B \rightarrow D\ell\nu_\ell)$, $\ell = e, \mu$, with small hadronic uncertainties. In the Standard Model one finds $R = 0.31 \pm 0.02$, $\mathcal{B}(B^- \rightarrow D^0\tau^-\bar{\nu}_\tau) = (0.71 \pm 0.09)\%$ and $\mathcal{B}(\bar{B}^0 \rightarrow D^+\tau^-\bar{\nu}_\tau) = (0.66 \pm 0.08)\%$, if the vector form factor of the Heavy Flavor Averaging Group is used. $B \rightarrow D\tau\nu_\tau$ is competitive with $B^+ \rightarrow \tau^+\nu_\tau$ in the search for effects of charged Higgs bosons. Especially sensitive to the latter is the differential distribution in the decay chain $\bar{B} \rightarrow D\bar{\nu}_\tau\tau^- [\rightarrow \pi^-\nu_\tau]$.

1. Higgs effects in B physics

Weakly-coupled extensions of the Standard Model (SM) typically possess a richer Higgs sector than the latter. The easiest extension of the SM Higgs sector involves one additional Higgs doublet and is realised in the Minimal Supersymmetric Standard Model (MSSM). At tree-level the MSSM Higgs sector coincides with a Two-Higgs-doublet model (2HDM) of type II, in which down-type fermions receive their masses solely from one doublet, while up-type fermion masses exclusively stem from Yukawa interactions with the other Higgs doublet. An important parameter is the ratio $\tan\beta$ of the two vacuum expectation values. In the type-II 2HDM the bottom and top Yukawa couplings y_b and y_t satisfy the relation

$$\frac{y_b}{y_t} = \frac{m_b}{m_t} \tan\beta.$$

Values around $\tan\beta = \mathcal{O}(60)$ correspond to y_b - y_t unification, which occurs in grand-unified theories (GUTs) with a minimal Yukawa sector. The idea of grand unification seems to call for low-energy supersymmetry, which stabilises the electroweak scale against radiative corrections from heavy GUT particles, improves the unification of

the gauge couplings and reconciles the prediction of the proton lifetime with its experimental bounds. Probing the large- $\tan\beta$ region of the MSSM is therefore of great interest, since the question of Yukawa unification sheds light on the Yukawa sector of the underlying GUT theory. Yet large values of $\tan\beta$ are also interesting from purely phenomenological considerations: The tension between the measured anomalous magnetic moment of the muon, a_μ [1], and the Standard Model prediction [2] invites supersymmetry with $\tan\beta \gtrsim 10$, and larger values of $\tan\beta$ allow to saturate a_μ with heavier superpartners. Recent global fits of electroweak and B-physics observables to the constrained MSSM and the model with minimal gauge-mediated supersymmetry breaking gave best fits for values of $\tan\beta = 54$ and $\tan\beta = 55$, respectively [3].

B physics is excellently suited to study large- $\tan\beta$ scenarios, because down-type Yukawa couplings grow with $\tan\beta$ and $\tan\beta = \mathcal{O}(50)$ corresponds to $y_b \sim 1$ [4]. Most dramatic effects can be expected in the leptonic decays $B_q \rightarrow \ell^+\ell^-$ (with $q = d$ or s and $\ell = e, \mu$ or τ), which are not only loop-suppressed in the Standard Model but also suffer from an additional helicity suppression. In particular the 95% CL limit

$$\begin{aligned} \mathcal{B}(B_s \rightarrow \mu^+\mu^-) &\leq 5.8 \cdot 10^{-8} \\ &\approx 18 \cdot \mathcal{B}^{\text{SM}}(B_s \rightarrow \mu^+\mu^-) \end{aligned}$$

*Talk at *Second Workshop on Theory, Phenomenology and Experiments in Heavy Flavour Physics*, June 16-18 2008, Anacapri, Italy. Work supported by DFG grant NI 1105/1-1, SFB-TR09 and the EU Contract MRTN-CT-2006-035482, "FLAVIANet".

from the CDF experiment [5] already cuts into the large- $\tan\beta$ region of the MSSM parameter space [4]. This is even true for the popular scenario of Minimal Flavour Violation (MFV) [6], in which the supersymmetric contribution to the $B_s \rightarrow \mu^+\mu^-$ amplitude involves the same elements of the Cabibbo-Kobayashi-Maskawa (CKM) matrix as the SM amplitude. For large $\tan\beta$ one finds

$$\mathcal{B}(B_s \rightarrow \mu^+\mu^-) \propto \epsilon_Y^2 \frac{\tan^6\beta}{M_{A^0}^4}, \quad (1)$$

where M_{A^0} is the mass of the CP-odd Higgs boson and ϵ_Y is a loop function which depends on several MSSM parameters [4]. The pattern of Eq. (1) is in sharp contrast with the case of the naive type-II 2HDM, in which $\mathcal{B}(B_s \rightarrow \mu^+\mu^-)$ is proportional to only four powers of $\tan\beta$ [7]. In the LHCb experiment it will be possible to measure $\mathcal{B}(B_s \rightarrow \mu^+\mu^-)$ for any value of $\tan\beta$. One can then test the MFV hypothesis by checking whether $\mathcal{B}(B_d \rightarrow \mu^+\mu^-)/\mathcal{B}(B_s \rightarrow \mu^+\mu^-)$ agrees with $|V_{td}/V_{ts}|^2 f_{B_d}^2/f_{B_s}^2$, where f_{B_q} is the decay constant of the B_q meson.

Due to the overall loop factor of ϵ_Y the bound on $\tan^3\beta/M_{A^0}^2$ derived from Eq. (1) depends on a plethora of other MSSM parameters. By contrast, effects of the charged Higgs boson H^+ enter B decays at the tree-level. The information gained from charged-Higgs-mediated processes is therefore more directly related to the parameters of the MSSM Higgs sector, with smaller dependences on e.g. superpartner masses. H^+ effects are best studied in leptonic and semi-leptonic B decays, in which hadronic uncertainties are under sufficient control. We specify our discussion to the case of a τ lepton in the final state, because the Yukawa couplings of the third fermion generation are largest. The B factories have observed the decay $B \rightarrow \tau\nu$ with [8]

$$\mathcal{B}(B \rightarrow \tau\nu) = (1.41 \pm 0.43) \times 10^{-4}, \quad (2)$$

which allows to place first useful constraints on $\tan\beta/M_{H^+}$ [9]. In the following sections I will elaborate on another promising charged-Higgs hunting ground, the decay $B \rightarrow D\tau\nu$, and compare this mode with $B \rightarrow \tau\nu$. The presented work has been performed in collaboration with Stéphanie Trine and Susanne Westhoff [10].

2. Charged-Higgs effects at large $\tan\beta$

The $\bar{q}bH^+$ coupling (with $q = u$ or c) is given by

$$\mathcal{L}_{\bar{q}bH^+} = -\frac{g}{2\sqrt{2}} \frac{\bar{m}_b}{M_W} \frac{\tan\beta}{1 + \epsilon_b \tan\beta} V_{qb} \cdot \bar{q}(1 + \gamma_5)bH^+, \quad (3)$$

where the small Yukawa coupling y_q is set to zero. The bottom quark mass \bar{m}_b is defined in the same QCD renormalisation scheme as the current $\bar{q}(1 + \gamma_5)b$. In the 2HDM of type-II the parameter ϵ_b vanishes. In the MSSM with MFV ϵ_b is a loop factor; the typically dominant squark-gluino contribution to ϵ_b is proportional to $\mu^*/M_{\tilde{g}}$, where μ is the Higgsino mass parameter and $M_{\tilde{g}}$ is the gluino mass [4]. A priori ϵ_b could be complex, but experimental constraints from electric dipole moments severely constrain the phase of $\mu^*/M_{\tilde{g}}$ and thereby of ϵ_b . Since $|\epsilon_b|\tan\beta$ can be of order 1, the charged-Higgs phenomenology does involve genuine supersymmetric parameters, yet with much less impact than in $B_s \rightarrow \mu^+\mu^-$. In the MSSM with a generic flavour structure ϵ_b is different for $q = u$ and $q = c$ and may obtain a sizable phase. In the generic 2HDM ϵ_b is generated at tree-level and is typically complex. For an early extensive study of $B \rightarrow D\ell\nu_\ell$ and $B \rightarrow D\tau\nu_\tau$ in the MFV-MSSM see Ref. [11].

The effective hamiltonian describing $b \rightarrow q\tau\nu$ transitions mediated by W^+ or H^+ can be written as

$$H_{\text{eff}} = \frac{G_F}{\sqrt{2}} V_{qb} \left\{ \bar{q}\gamma^\mu(1 - \gamma_5)b \bar{\tau}\gamma_\mu(1 - \gamma_5)\nu_\tau - \frac{\bar{m}_b m_\tau}{m_B^2} \bar{q} [g_S + g_P \gamma_5] b \bar{\tau}(1 - \gamma_5)\nu_\tau \right\} + \text{h.c.} \quad (4)$$

In the MSSM the effective couplings g_S and g_P read

$$g_S = g_P = \frac{m_B^2}{M_{H^+}^2} \frac{\tan^2\beta}{(1 + \epsilon_b \tan\beta)(1 + \epsilon_\tau \tan\beta)}. \quad (5)$$

Here ϵ_τ is the analogue of ϵ_b for the $\bar{\nu}_\tau\tau H^+$ coupling. $B^+ \rightarrow \tau^+\nu$ probes the coupling g_P [9]:

$$\mathcal{B}(B^+ \rightarrow \tau^+\nu) \propto |V_{ub}|^2 f_B^2 |1 - g_P|^2 \quad (6)$$

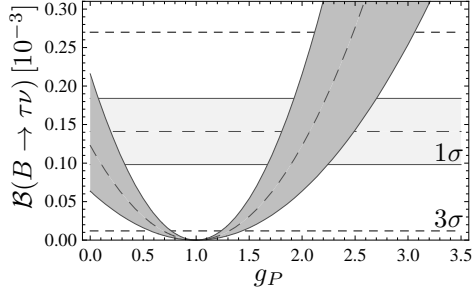


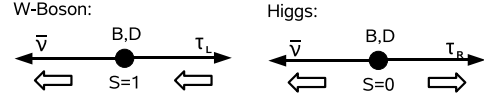
Figure 1. $\mathcal{B}(B^+ \rightarrow \tau^+ \nu)$ vs. g_P for real g_P .

The B meson decay constant $f_B = 216 \pm 38$ MeV [13] is the dominant source of theoretical uncertainty in the extraction of $|1 - g_P|$ from $\mathcal{B}(B^+ \rightarrow \tau^+ \nu)$. Eq. (6) is confronted with the experimental result of Eq. (2) in Fig. 1.

The semi-tauonic decay $B \rightarrow D\tau\nu_\tau$ instead probes the coupling g_S , because B and D have the same parity. In the MFV-MSSM $B \rightarrow D\tau\nu_\tau$ and $B^+ \rightarrow \tau^+\nu$ probe the same parameters, because ϵ_b in Eqs. (3) and (5) is the same for $b \rightarrow u$ and $b \rightarrow c$ transitions. Thus within the MFV-MSSM we can combine the information from both decay modes to constrain the combination of $\tan\beta$, M_{H^\pm} , ϵ_b and ϵ_τ in Eq. (5). If new physics is found, a comparison of g_S extracted from $B \rightarrow D\tau\nu_\tau$ with g_P obtained from $B^+ \rightarrow \tau^+\nu$ will probe physics beyond the MFV-MSSM. $B \rightarrow D\tau\nu$ compares to $B^+ \rightarrow \tau^+\nu$ as follows:

- i) $\mathcal{B}(B \rightarrow D\tau\nu_\tau) \approx 50 \mathcal{B}(B^+ \rightarrow \tau^+\nu_\tau)$.
- ii) $|V_{cb}|$ entering $B \rightarrow D\tau\nu_\tau$ is much better known than $|V_{ub}|$.
- iii) The uncertainty in lattice calculations of f_B^2 needed for $B \rightarrow \tau\nu_\tau$ is 30%. Instead $B \rightarrow D\tau\nu$ involves hadronic form factors. We will see below in Sect. 3 that the associated theoretical uncertainty is smaller, if experimental data on $B \rightarrow D\ell\nu_\ell$ with $\ell = e, \mu$ are exploited.
- iv) The three-body decay $B \rightarrow D\tau\nu_\tau$ has decay distributions which discriminate between W^+ and H^+ exchange.
- v) $B \rightarrow \tau\nu_\tau$ is mildly helicity-suppressed. In $B \rightarrow D\tau\nu_\tau$ the (transverse) W^+

contribution is helicity suppressed in the kinematic region with slow D meson (P-wave suppression) [14]:



3. Charged-Higgs effects in $B \rightarrow D\tau\nu_\tau$

$B \rightarrow D\ell\nu_\ell$, $\ell = e, \mu, \tau$, involves the hadronic matrix elements of the vector current and of the scalar current, which are expressed in terms of two form factors,[†] V_1 and S_1 :

$$\begin{aligned} \langle D(p_D) | \bar{c} \gamma^\mu b | \bar{B}(p_B) \rangle &= \\ V_1(w) \frac{m_B + m_D}{2\sqrt{m_B m_D}} \left[p_B^\mu + p_D^\mu - \frac{m_B^2 - m_D^2}{q^2} q^\mu \right] \\ &+ S_1(w) (1+w) \sqrt{m_B m_D} \frac{m_B - m_D}{q^2} q^\mu \\ \langle D(p_D) | \bar{c} b(\mu) | \bar{B}(p_B) \rangle &= \\ S_1(w) (1+w) \sqrt{m_B m_D} \frac{m_B - m_D}{\bar{m}_b(\mu) - \bar{m}_c(\mu)}, \quad (7) \end{aligned}$$

where m_D and m_B are the meson masses, $q = p_B - p_D$ is the momentum transfer and the running quark masses \bar{m}_b and \bar{m}_c are evaluated at the renormalisation scale μ at which the scalar current $\bar{c}b$ is defined. The kinematic variable

$$w = \frac{m_B^2 + m_D^2 - q^2}{2m_D m_B} \quad (8)$$

is defined in such a way that the kinematic endpoint $q^2 = (m_B - m_D)^2$ corresponds to $w = 1$. Heavy quark symmetry implies [15]

$$S_1(1) = V_1(1) = 1 + \mathcal{O}(1/m_c, \alpha_s). \quad (9)$$

For $m_\ell = 0$ the other kinematic endpoint is at $q^2 = 0$ corresponding to $w_{\max} = (m_B^2 + m_D^2)/(2m_D m_B) = 1.59$. The absence of a pole at $q^2 = 0$ in Eq. (7) implies

$$S_1(w_{\max}) = V_1(w_{\max}). \quad (10)$$

The next step towards a precision analysis of $B \rightarrow D\tau\nu_\tau$ exploits the analyticity properties of form factors [16]: The location of poles and

[†]There is a typo in the definition of S_1 in Ref. [10].

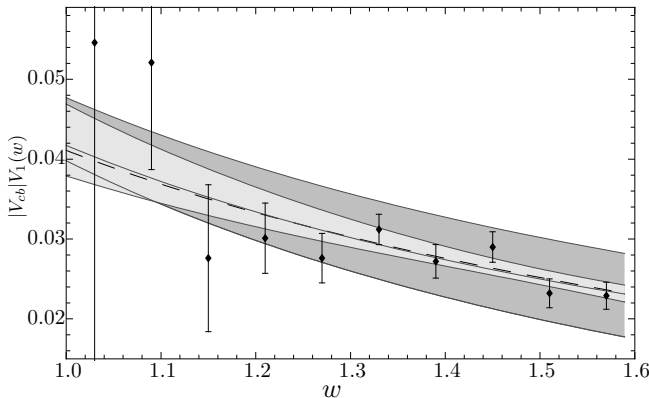


Figure 2. Vector form factor $V_1(w)$. Dots: BELLE data on $B \rightarrow D\ell\nu_\ell$ [17] with statistical errors only. Dark gray band: form factor from BELLE data with HQET constraint at $w = 1$ (systematic errors dominate at large recoil). Light gray band: form factor from HFAG, which includes older CLEO and ATLAS data [18]. Solid line: best fit of BELLE data to a_0^V and a_1^V . Dashed line: best fit of Ref. [17] (using different parameters).

branch points in V_1 and S_1 can be inferred from the particle spectrum. The conformal mapping

$$z = \frac{\sqrt{(m_B + m_D)^2 - q^2} - \sqrt{(m_B + m_D)^2 - t_0}}{\sqrt{(m_B + m_D)^2 - q^2} + \sqrt{(m_B + m_D)^2 - t_0}}$$

and the elimination of subthreshold poles renders the form factors analytic in the new variable z in the entire kinematic region (see [16,10] for details). That is, we can parameterise V_1 and S_1 in terms of power series in z . With a proper choice of the free parameter t_0 the kinematic range $1 \leq w \leq 1.59$ is mapped onto $0 \leq |z| \leq 0.032$. $B \rightarrow D\ell\nu_\ell$ with $\ell = e, \mu$ only involves V_1 . We can use experimental data to verify that the first two coefficients a_0^V and a_1^V of the power series are sufficient to describe the normalisation and shape of V_1 . Moreover, the dependence on a_1^V is moderate. The result is shown in Fig. 2. Finally we need the scalar form factor $S(w)$. The corresponding parameters a_0^S and a_1^S are fixed through Eqs. (9) and (10), using the $1/m_c$ and α_s corrections from [19]. An alternative approach uses lattice data to fix the form factors near $w = 1$

[20]. Note that our analysis faces much smaller hadronic uncertainties than the extraction of $|V_{cb}|$ from $B \rightarrow D\ell\nu_\ell$: We first fix $|V_{cb}|V_1(w)$ from experiment. Then Eq. (10) determines the normalisation of $|V_{cb}|S_1(w)$ in terms of measured quantities. Keeping only a_0^S already reproduces $S(w)$ to 90%, and neither hadronic uncertainties nor the error in $|V_{cb}|$ have entered the prediction of $B \rightarrow D\tau\nu_\tau$ yet. Hadronic uncertainties only enter when we increase the accuracy further and fix the slope parameter a_1^S by including Eq. (9). These uncertainties are suppressed by $1/m_c$. In this step one also needs the experimental value of $|V_{cb}|$, whose error is around 2%. A remaining source of hadronic uncertainty is the next term a_2^S of the series in z . In the data for V_1 in Fig. 2 we found the influence of a_2^V negligible[‡] and expect the same behaviour for a_2^S and S_1 .

The first application of our analysis in [10] is a new prediction of branching fractions in the SM:

$$\begin{aligned} \mathcal{B}(B^- \rightarrow D^0 \tau^- \bar{\nu}_\tau) &= (0.71 \pm 0.09)\% \\ \mathcal{B}(\bar{B}^0 \rightarrow D^+ \tau^- \bar{\nu}_\tau) &= (0.66 \pm 0.08)\% \\ R \equiv \frac{\mathcal{B}(B \rightarrow D\tau\nu_\tau)}{\mathcal{B}(B \rightarrow D\ell\nu_\ell)} &= 0.31 \pm 0.02 \end{aligned} \quad (11)$$

using the HFAG form factor V_1 [18]. Note the small uncertainty in R which is the relevant quantity for charged-Higgs hunting. This has to be compared with the $\mathcal{O}(40\%)$ error of $|V_{ub}|^2 f_B^2$ entering the SM prediction of $B \rightarrow \tau\nu_\tau$. The uncertainties in Eq. (11) will decrease further with better data on $B \rightarrow D\ell\nu_\ell$. The dependence of R on g_S is shown in Fig. 3. A home-use formula for R as a function of g_S can be found in Eq. (7) of Ref. [10]. We notice that the dependence of R on g_S is weaker than the dependence of $\mathcal{B}(B^+ \rightarrow \tau^+ \nu)$ on g_P , but the present 1σ upper bounds on the effective coupling constants are similar. However, if nature has opted for a large charged-Higgs contribution suppressing R to values below 0.2, it will not be easy to determine g_S because the curve in Fig. 3 is quite flat. At present there is also an open experimental issue in $B \rightarrow D\tau\nu_\tau$: The Monte Carlo simulations

[‡]For a lattice study of a_2^V in the $B \rightarrow \pi$ form factor, which involves the much larger range $0 \leq |z| \leq 0.28$ than our $B \rightarrow D$ transition, see Paul Mackenzie's talk at this conference.

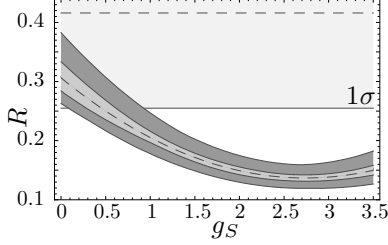


Figure 3. $R \equiv \mathcal{B}(B \rightarrow D\tau\nu_\tau)/\mathcal{B}(B \rightarrow D\ell\nu_\ell)$ as a function of g_S . Light gray band: $R^{\text{exp}} = 0.416 \pm 0.117 \pm 0.052$ [21]. Dark gray band: R computed with BELLE form factor V_1 [17]. Gray band: R computed with HFAG form factor V_1 [18].

use the SM formula for the decay distribution in $B \rightarrow D\tau\nu_\tau$, but the D energy is higher on average if a charged-Higgs contribution is present, because there is a destructive interference with the longitudinal W boson contribution. The efficiencies for D detection are smaller for very soft D 's, which may affect the upper bound on g_S derived from R^{exp} .

It is well known that the sensitivity of $B \rightarrow D\tau\nu_\tau$ to charged-Higgs effects is improved, if information on the τ polarisation is included [22]. However, in B factories the τ is too slow to decay with a displaced vertex, so that the τ kinematics is not accessible to experiment. To my knowledge, the only theory paper addressing this problem is Ref. [23], which proposes to study the differential decay rate $d\Gamma/dE_D$, where E_D is the D meson energy in the B rest frame. We have studied the decay chain $\bar{B} \rightarrow D\bar{\nu}_\tau\tau^-$ with the subsequent decay $\tau^- \rightarrow \pi^-\nu_\tau$ and propose to study the triple differential decay rate $d\Gamma/(dE_D dE_\pi d\cos\theta)$, where E_π is the π^- energy and θ is the angle between the three-momenta of the D and the π^- . This quantity not only discriminates between SM and charged-Higgs effects in an excellent way, it also allows to constrain the phase of g_S . This feature is illustrated in Fig. 4.

Acknowledgements

I am grateful to Stéphanie Trine and Susanne Westhoff for an enjoyable collaboration and thank them for proofreading. Stimulating discussions

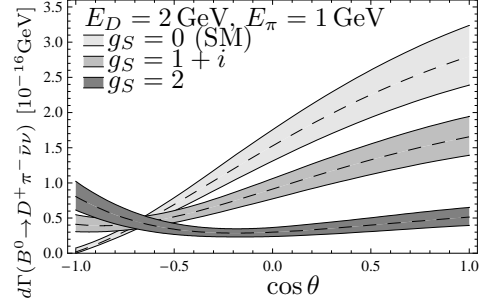


Figure 4. Angular distribution for $E_D = 2$ GeV and $E_\pi = 1$ GeV and $g_S = 0, 1 + i, 2$. In models with $g_P = g_S$ these three values correspond to the same $\mathcal{B}(B^+ \rightarrow \tau^+\nu)$.

with Christoph Schwanda on experimental issues are gratefully acknowledged.

REFERENCES

1. G. W. Bennett [Muon Collaboration], Phys. Rev. D **73** (2006) 072003.
2. J. P. Miller, E. de Rafael and B. L. Roberts, Rept. Prog. Phys. **70** (2007) 795. F. Jegerlehner, arXiv:hep-ph/0703125; K. Hagiwara, A. D. Martin, D. Nomura and T. Teubner, Phys. Lett. B **649** (2007) 173. and references therein.
3. S. Heinemeyer, X. Miao, S. Su and G. Weiglein, arXiv:0805.2359 [hep-ph].
4. C. Hamzaoui, M. Pospelov and M. Toharia, Phys. Rev. D **59** (1999) 095005 [arXiv:hep-ph/9807350]. K. S. Babu and C. F. Kolda, Phys. Rev. Lett. **84** (2000) 228 [arXiv:hep-ph/9909476]. C. S. Huang, W. Liao, Q. S. Yan and S. H. Zhu, Phys. Rev. D **63** (2001) 114021 [Erratum-ibid. D **64** (2001) 059902] [arXiv:hep-ph/0006250]. M. S. Carena, D. Garcia, U. Nierste and C. E. M. Wagner, Phys. Lett. B **499**, 141 (2001) [arXiv:hep-ph/0010003]. A. Dedes, H. K. Dreiner and U. Nierste, Phys. Rev. Lett. **87** (2001) 251804 [arXiv:hep-ph/0108037]. G. Isidori and A. Retico, JHEP **0111** (2001) 001 [arXiv:hep-ph/0110121]. A. Dedes, H. K. Dreiner, U. Nierste and P. Richardson, arXiv:hep-ph/0207026. A. J. Buras,

- P. H. Chankowski, J. Rosiek and L. Slawianowska, Nucl. Phys. B **659** (2003) 3 [arXiv:hep-ph/0210145]. A. J. Buras, P. H. Chankowski, J. Rosiek and L. Slawianowska, Phys. Lett. B **546** (2002) 96 [arXiv:hep-ph/0207241]. A. G. Akeroyd and S. Recksiegel, J. Phys. G **29** (2003) 2311 [arXiv:hep-ph/0306037]. M. S. Carena, A. Menon, R. Noriega-Papaqui, A. Szynekman and C. E. M. Wagner, Phys. Rev. D **74** (2006) 015009 [arXiv:hep-ph/0603106]. S. Trine, arXiv:0710.4955 [hep-ph].
5. T. Aaltonen *et al.* [CDF Collaboration], Phys. Rev. Lett. **100** (2008) 101802 [arXiv:0712.1708 [hep-ex]]. Adding the limit from the DØ experiment, V. M. Abazov *et al.* [D0 Collaboration], Phys. Rev. D **76** (2007) 092001 [arXiv:0707.3997 [hep-ex]], improves the CDF limit only marginally. See also: T. Kuhr [CDF Collaboration and D0 Collaboration], arXiv:0804.2743 [hep-ex]. The SM value has been computed to next-to-leading order in QCD in: G. Buchalla and A. J. Buras, Nucl. Phys. B **400** (1993) 225. A numerical update can be found in: M. Artuso *et al.*, “*B, D and K decays*”, *Report of Working Group 2 of the CERN Workshop on Flavor in the Era of the LHC*, Geneva, Switzerland, 6-8 Feb 2006, arXiv:0801.1833 [hep-ph].
 6. G. D’Ambrosio, G. F. Giudice, G. Isidori and A. Strumia, Nucl. Phys. B **645** (2002) 155 [arXiv:hep-ph/0207036].
 7. H. E. Logan and U. Nierste, Nucl. Phys. B **586**, 39 (2000) [arXiv:hep-ph/0004139].
 8. BELLE Collaboration, Phys. Rev. Lett. **97**, 251802 (2006); BABAR Collaboration, Phys. Rev. D **76**, 052002 (2007); average: D. Monorchio, talk presented at HEP2007, <http://www.hep.man.ac.uk/HEP2007/>.
 9. W. Hou, Phys. Rev. D **48**, 2342 (1993). G. Isidori and P. Paradisi, Phys. Lett. B **639** (2006) 499 [arXiv:hep-ph/0605012].
 10. U. Nierste, S. Trine and S. Westhoff, Phys. Rev. D **78** (2008) 015006, [arXiv:0801.4938 [hep-ph]].
 11. H. Itoh, S. Komine and Y. Okada, Prog. Theor. Phys. **114** (2005) 179 [arXiv:hep-ph/0409228].
 12. M. Carena, M. Olechowski, S. Pokorski and C.E.M. Wagner, Nucl. Phys. B **426** (1994) 269; L.J. Hall, R. Rattazzi and U. Sarid, Phys. Rev. D **50** (1994) 7048. T. Blazek, S. Raby and S. Pokorski, Phys. Rev. D **52** (1995) 4151 [arXiv:hep-ph/9504364]. M. S. Carena, D. Garcia, U. Nierste and C. E. M. Wagner, Nucl. Phys. B **577** (2000) 88 [arXiv:hep-ph/9912516].
 13. M. Della Morte, PoS LAT2007, 8.
 14. B. Grzadkowski and W. Hou, Phys. Lett. B **283**, 427 (1992). R. Garisto, Phys. Rev. D **51** (1995) 1107 [arXiv:hep-ph/9403389]. For studies of inclusive $B \rightarrow X\tau\nu$ decays see: J. Kalinowski, Phys. Lett. B **245** (1990) 201.
 15. N. Isgur and M.B. Wise, Phys. Lett. B **232**, 113 (1989); **237**, 527 (1990); B. Grinstein, Nucl. Phys. B **339**, 253 (1990); E. Eichten and B. Hill, Phys. Lett. B **234**, 511 (1990); H. Georgi, Phys. Lett. B **240**, 447 (1990).
 16. C. Bourrely, B. Machet and E. de Rafael, Nucl. Phys. B **189** (1981) 157. C. G. Boyd and M. J. Savage, Phys. Rev. D **56** (1997) 303 [arXiv:hep-ph/9702300]. C.G. Boyd, B. Grinstein and R.F. Lebed, Phys. Rev. D **56**, 6895 (1997). I. Caprini, L. Lellouch and M. Neubert, Nucl. Phys. B **530**, 153 (1998). R. Hill, [hep-ph/0606023].
 17. BELLE Collaboration, Phys. Lett. B **526**, 258 (2002).
 18. Heavy Flavor Averaging Group, [0704.3575][hep-ex], and online update at <http://www.slac.stanford.edu/xorg/hfag/>.
 19. Z. Ligeti, Y. Nir and M. Neubert, Phys. Rev. D **49**, 1302 (1994). M. Neubert, Phys. Rev. D **46**, 2212 (1992).
 20. J.F. Kamenik and F. Mescia, Phys. Rev. D **78** (2008) 014003 [arXiv:0802.3790 [hep-ph]].
 21. BABAR Collaboration, Phys. Rev. Lett. **100**, 021801 (2008).
 22. M. Tanaka, Z. Phys. C **67**, 321 (1995). Within the SM τ polarisation effects are analysed in: K. Hagiwara, A. D. Martin and M. F. Wade, Z. Phys. C **46** (1990) 299.
 23. K. Kiers and A. Soni, Phys. Rev. D **56**, 5786 (1997).